Inorg. Chem. **2008**, *47*, 5197−5203

Inorganic Chemistry
Article

Self-Assembly of a Copper(II)-Based Metallosupramolecular Hexagon

Eugenio Coronado,* José Ramón Galan-Mascaros, Pablo Gaviña,* Carlos Martí-Gastaldo,
Francisco M. Romero, and Sergio Tatay

Instituto de Ciencia Molecular and Fundación General de la UVEG, Universidad de Valencia;
Polígono la Coma s/n, 46980-Paterna (Valencia), Spain

Received January 11, 2008

The self-assembly of a 1:1 mixture of copper(II) ions and a rigid heteroditopic ligand **L** containing phen and terpy binding units gives rise in the solid state to green crystals of a hexanuclear metallamacrocycle **1**. X-ray crystallography reveals that **1** consists of molecular hexagons of the grid-type family in which each metal ion is bound to two different ligands through the phen and terpy units, plus a weakly coordinated PF_6^- anion in a highly distorted octahedral geometry. ES-MS studies of acetonitrile solutions of **L** and copper(II) in a 1:1 ratio show mixtures of polynuclear complexes in which trinuclear $\mathbf{L}_3Cu_3$ species are predominant.

Introduction

Metallosupramolecular chemistry uses self-assembly processes between organic ligands and metal ions to construct multicomponent and multinuclear coordination entities.[1] Discrete 2D assemblies displaying closed superstructures incorporating metal ions are known as metallamacrocycles. A wide variety of such complexes has been identified: from complexes having a distinctively geometric shape, the so-called molecular polygons, such as molecular triangles,[2–4] squares,[5–9] pentagons[10–12] or hexagons,[13–16] to assemblies like the circular helicates,[17–19] whose closed cyclic nature is the only distinguishing feature.[20–22] The investigation of such self-assemblies is of interest from a fundamental point of view because it contributes to the understanding of how to access unique supramolecular architectures with well-defined shapes and geometries at the nanometer scale that are practically inaccessible by other means.

Two outstanding strategies have been developed for the self-assembly of molecular polygons (Table 1). Both approaches usually rely on the use of relatively rigid ditopic ligands bearing nitrogen donor atoms (although oxygen-, sulfur-, or phosphorus-containing ligands have also been reported) and complex species with coordinatively unsaturated metal ions or with easily accessible coordination sites.

---

* To whom correspondence should be addressed. E-mail: pablo.gavina@uv.es. Fax: 34 963543273. Phone: 34 963544421.

(1) Lehn, J.-M., *Supramolecular Chemistry: Concepts and Perspectives*; VCH: Weinheim, Cambridge, 1995; p 271.

(2) Cotton, F. A.; Daniels, L. M.; Lin, C.; Murillo, C. A. *J. Am. Chem. Soc.* **1999**, *121*, 4538–4539.

(3) Cotton, F. A.; Murillo, C. A.; Yu, R. M. *Dalton Trans.* **2006**, 3900–3905.

(4) Hwang, S. H.; Moorefield, C. N.; Fronczek, F. R.; Lukoyanova, O.; Echegoyen, L.; Newkome, G. R. *Chem. Commun.* **2005**, 713–715.

(5) Fujita, M.; Yazaki, J.; Ogura, K. *J. Am. Chem. Soc.* **1990**, *112*, 5645–5647.

(6) Youinou, M. T.; Rahmouni, N.; Fischer, J.; Osborn, J. A. *Angew. Chem., Int. Ed. Engl.* **1992**, *31*, 733–735.

(7) Stang, P. J.; Cao, D. H. *J. Am. Chem. Soc.* **1994**, *116*, 4981–4982.

(8) Stang, P. J.; Olenyuk, B. *Angew. Chem., Int. Ed. Engl.* **1996**, *35*, 732–736.

(9) Cotton, F. A.; Lin, C.; Murillo, C. A. *J. Am. Chem. Soc.* **2001**, *123*, 2670–2671.

(10) Campos-Fernandez, C. S.; Clerac, R.; Koomen, J. M.; Russell, D. H.; Dunbar, K. R. *J. Am. Chem. Soc.* **2001**, *123*, 773–774.

(11) Campos-Fernandez, C. S.; Schottel, B. L.; Chifotides, H. T.; Bera, J. K.; Bacsa, J.; Koomen, J. M.; Russell, D. H.; Dunbar, K. R. *J. Am. Chem. Soc.* **2005**, *127*, 12909–12923.

(12) Hwang, S. H.; Wang, P. S.; Moorefield, C. N.; Godinez, L. A.; Manriquez, J.; Bustos, E.; Newkome, G. R. *Chem. Commun.* **2005**, 4672–4674.

(13) Newkome, G. R.; Cho, T. J.; Moorefield, C. N.; Baker, G. R.; Cush, R.; Russo, P. S. *Angew. Chem., Int. Ed.* **1999**, *38*, 3717–3721.

(14) Hall, J. R.; Loeb, S. J.; Shimizu, G. K. H.; Yap, G. P. A. *Angew. Chem., Int. Ed.* **1998**, *37*, 121–123.

(15) Stang, P. J.; Persky, N. E.; Manna, J. *J. Am. Chem. Soc.* **1997**, *119*, 4777–4778.

(16) Baxter, P. N. W.; Khoury, R. G.; Lehn, J. M.; Baum, G.; Fenske, D. *Chem.*−*Eur. J.* **2000**, *6*, 4140–4148.

(17) Hasenknopf, B.; Lehn, J. M.; Kneisel, B. O.; Baum, G.; Fenske, D. *Angew. Chem., Int. Ed. Engl.* **1996**, *35*, 1838–1840.

(18) Hasenknopf, B.; Lehn, J. M.; Boumediene, N.; DupontGervais, A.; VanDorsselaer, A.; Kneisel, B.; Fenske, D. *J. Am. Chem. Soc.* **1997**, *119*, 10956–10962.

(19) Mamula, O.; von Zelewsky, A.; Bernardinelli, G. *Angew. Chem., Int. Ed.* **1998**, *37*, 290–293.

(20) Mezei, G.; Baran, P.; Raptis, R. G. *Angew. Chem., Int. Ed.* **2004**, *43*, 574–577.

(21) Halper, S. R.; Cohen, S. M. *Angew. Chem., Int. Ed.* **2004**, *43*, 2385–2388.

(22) Mohamed, A. A.; Burini, A.; Galassi, R.; Paglialunga, D.; Galan-Mascaros, J. R.; Dunbar, K. R.; Fackler, J. P. *Inorg. Chem.* **2007**, *46*, 2348–2349.

10.1021/ic8000569 CCC: $40.75

Table 1. Strategies for the Self-Assembly of Molecular Polygons

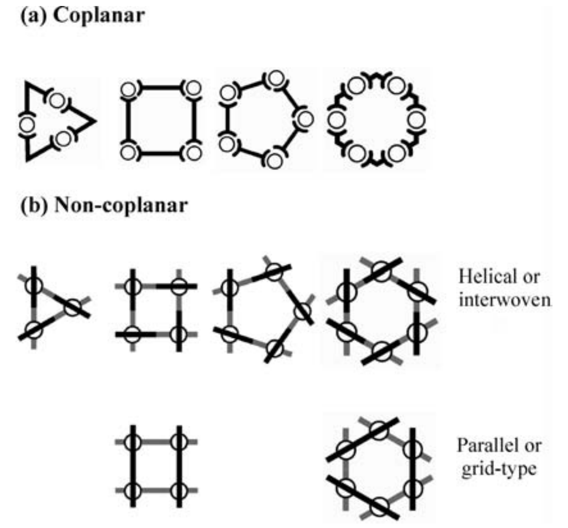

What makes the difference between both approaches is the way in which the ligand planes and the metal centers are related to each other. In the first one, all of the ligands and the metal centers lay on the same plane, and both the transition-metal coordination geometry and the predetermined angle between the binding units located at both ends of the organic ligand can be used to direct the metallamacrocyclic structure (part a of Table 1). This strategy has been nicely exploited by the groups of Fujita, Stang, Newkome, and many others.[23–26] In the second approach, the ligands and the metal centers are non-coplanar, and linear rodlike ditopic ligands coordinate naked transition-metal ions in an intertwined situation.[27–29]

Depending on whether the coordinating sites of the ditopic ligands adopt a transoid or cisoid orientation, helical (interwoven) or parallel (grid-type) arrangements of the ligands are obtained (part b of Table 1). Examples of interwoven molecular polygons with three up to several edges have been described. Still, parallel or grid-type metallamacrocycles are not so usual, squares being by far the most common systems.[30,31] Examples are even scarcer when heteroditopic ligands are used.

Encouraged by the recent synthesis of a new azaaromatic heteroditopic ligand (**L**) based on a 3,5-connected phenanthroline/terpyridine conjugate,[32] we decided to test its capabilities for the design of new metallamacrocycles. The structure of the ligand is depicted in Chart 1. **L** is a highly preorganized linear ligand with a 2,2′:6′,2″-terpyridine (terpy) tridentate ligand and a 1,10-phenanthroline (phen) bidentate moiety directly connected to one another (from the 3-position of the phen to the 5-position of the terpy).

Chart 1. Ditopic Ligand **L** and phen and terpy Building Blocks

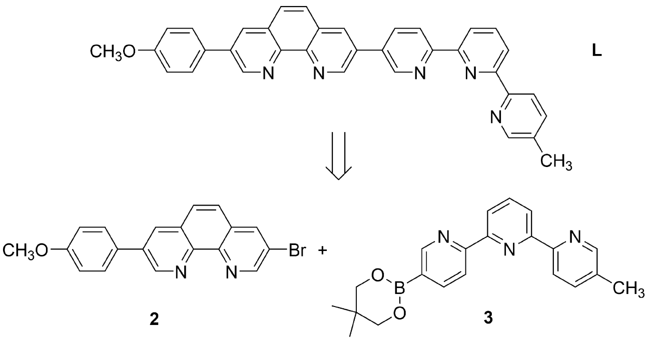

The fact that this ligand incorporates a bidentate and a tridentate moiety in principle reduces the scope of metals to be used to obtain a cyclic structure to those capable of pentacoordinate pyridine-type nitrogen donor ligands, such as copper, cobalt, zinc, or cadmium. In this sense, copper(II) seemed to be a good candidate because most of its complexes have a coordination number of 5 (square pyramidal geometries) or 6 (octahedral geometries, with Jahn–Teller distortion). Moreover, the ability of copper(II) to form 5-coordinate complexes involving both a phen and a terpy moiety has been previously exploited for the preparation of transition-metal-based molecular motors.[33] We describe herein the self-assembly in the solid state of a molecular hexagon **1** from copper(II) ions and the heteroditopic ligand **L**. Acetonitrile solutions of 1:1 mixtures of **L** and copper(II) have also been studied by ES-MS, and we have found that trimeric $\mathbf{L}_3\mathrm{Cu}_3$ species are predominant. UV–vis data, powder diffraction data, and magnetic susceptibility of the bulk polycrystalline sample are also reported.

Results and Discussion

L was synthesized in 67% yield by a Suzuki cross-coupling reaction between the bromo substituted phenanthroline **2** and the boronic ester derivative of the terpy **3** in the presence of $Pd(PPh_3)_4$ as catalyst and K_2CO_3 as a base (Chart 1).

The synthesis of the phen and terpy ligands is depicted in Scheme 1. 3-Bromo-8-(*p*-anisyl)-1,10-phenanthroline (**2**) was easily prepared in 56% yield from 3,8-dibromo-1,10-phenantroline (**4**)[34] and 4-methoxyphenylboronic acid neopentylglycol ester (**5**) under Suzuki cross-coupling conditions. On the other hand, a Stille-type cross-coupling reaction between 6′-bromo-5-methyl-2,2′-bipyridine (**6**) and 5-bromo-2-tributylstannylpyridine (**7**)[35] for 24 h in refluxing toluene afforded the monobromo-substituted terpyridine **8** in 82%

---

(23) Fujita, M. *Chem. Soc. Rev.* **1998**, *27*, 417–425.

(24) Leininger, S.; Olenyuk, B.; Stang, P. J. *Chem. Rev.* **2000**, *100*, 853–907.

(25) Newkome, G. R.; Cho, T. J.; Moorefield, C. N.; Cush, R.; Russo, P. S.; Godinez, L. A.; Saunders, M. J.; Mohapatra, P. *Chem.—Eur. J.* **2002**, *8*, 2946–2954.

(26) Romero, F. M.; Ziessel, R.; DupontGervais, A.; VanDorsselaer, A. *Chem. Commun.* **1996**, *551*, 553.

(27) Ruben, M.; Rojo, J.; Romero-Salguero, F. J.; Uppadine, L. H.; Lehn, J. M. *Angew. Chem., Int. Ed.* **2004**, *43*, 3644–3662.

(28) Bark, T.; von Zelewsky, A.; Rappoport, D.; Nenburger, M.; Schaffner, S.; Lacour, J.; Jodry, J. *Chem.—Eur. J.* **2004**, *10*, 4839–4845.

(29) Swiegers, G. F.; Malefetse, T. J. *Chem. Rev.* **2000**, *100*, 3483–3537.

(30) Würthner, F.; You, C. C.; Saha-Möller, C. R. *Chem. Soc. Rev.* **2004**, *33*, 133–146.

(31) Fujita, M.; Tominaga, M.; Hori, A.; Therrien, B. *Acc. Chem. Res.* **2005**, *38*, 371–380.

(32) Gaviña, P.; Tatay, S. *Tetrahedron Lett.* **2006**, *47*, 3471–3473.

(33) Collin, J. P.; Dietrich-Buchecker, C.; Gaviña, P.; Jimenez-Molero, M. C.; Sauvage, J. P. *Acc. Chem. Res.* **2001**, *34*, 477–487.

(34) Saitoh, Y.; Koizumi, T.; Osakada, K.; Yamamoto, T. *Can. J. Chem.* **1997**, *75*, 1336–1339.

(35) Wang, X.; Rabbat, P.; O'Shea, P.; Tillyer, R.; Grabowski, E. J. J.; Reider, P. J. *Tetrahedron Lett.* **2000**, *41*, 4335–4338.

Scheme 1. Reagents and Conditions: (i) $Pd(PPh_3)_4$, Na_2CO_3, Toluene−H_2O, Reflux (56%); (ii) $Pd(PPh_3)_4$, Toluene, Reflux (82%); (iii) bis(Neopentyl glycolato)diboron, $Pd(dppf)Cl_2$, KOAc, DMSO, 80 °C (65%)

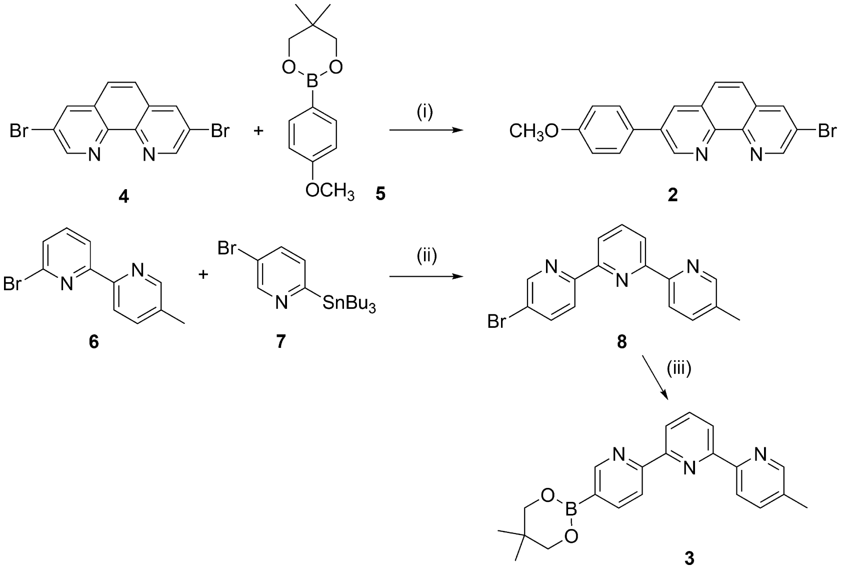

yield after chromatography. Finally, **8** was reacted with bis(neopentyl glycolato)diboron in DMSO in the presence of potassium acetate and a catalytic amount of $Pd(dppf)Cl_2$ to yield 5-(neopentyl glycolatoboron)-5″-methyl-2,2′:6′,2″-terpyridine **3** in 65% yield.

When a 1:1 stoichiometric mixture of **L** and $Cu(OAc)_2$ in methanol was stirred at room temperature, a bright-green solution was obtained within minutes. KPF_6 and water was added to the mixture, giving rise to a green powder in quantitative yield. This precipitate was collected and recrystallized from acetonitrile to yield green crystals suitable for X-ray diffraction of metallacycle **1**, along with some microcrystalline powder.

The crystal structure of $[\mathbf{1}][PF_6]_{12}$ contains the hexameric cation $[Cu_6(\mathbf{L})_6(PF_6)_6]^{6+}$. This cation is formed by six Cu^{2+} centers with [5 + 1] coordination (Figure 1). Each metal ion is bound to two different **L** ligands through the phen and terpy binding sites, plus a weakly coordinated PF_6^- anion that completes the highly distorted octahedral geometry. The equatorial positions are occupied by the terpy and one of the phen nitrogen atoms, with distances as short as 1.93 Å. These four equatorial sites are not perfectly coplanar with the copper atom, which appears to be about ∼0.16(2) Å deviated from the equatorial plane, toward the remaining nitrogen atom from the phen ligand, with a longer distance (2.20(6) Å), as expected for the elongated axis of the octahedron. The opposite site has a much longer distortion, with a Cu−F distance of 2.70(6) Å (Figure S1 in the Supporting Information).

As expected for grid-type metallacycles, the coordinating ligands are disposed in a cisoid fashion above and below the mean plane of the hexamer. Within each **L** unit, terpy and phen are twisted with a dihedral angle of 52.2°. The terpy and phen groups binding a copper atom belong to two

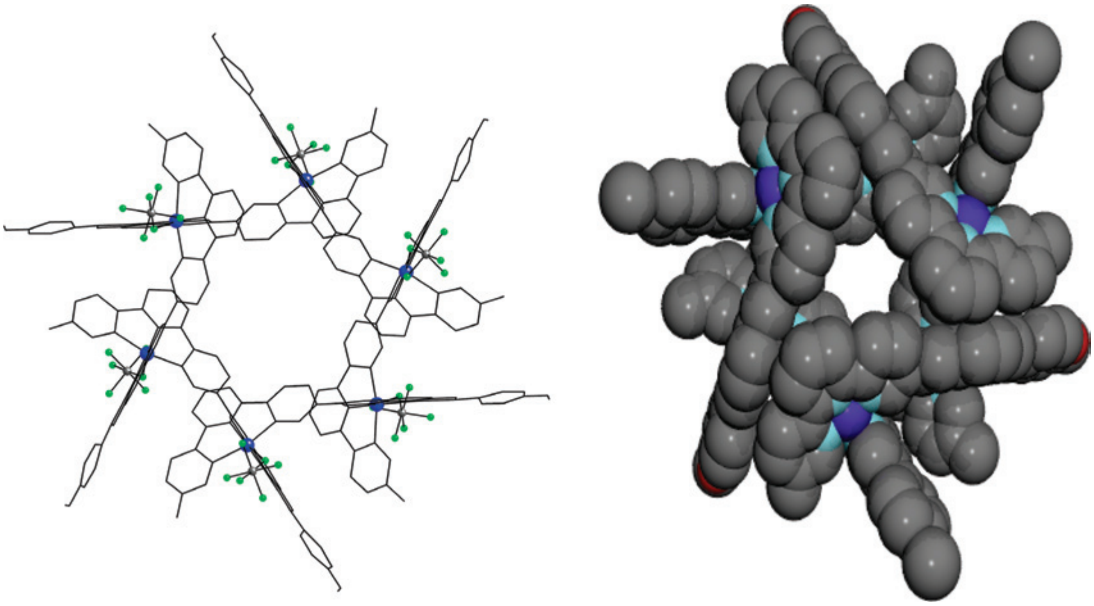

Figure 1. Top view of the $[Cu_6(\mathbf{L})_6(PF_6)_6]^{6+}$ ($[\mathbf{1}(PF_6)_6]^{6+}$) cation (left) and space-filling diagram of the molecular cation **1** (right).

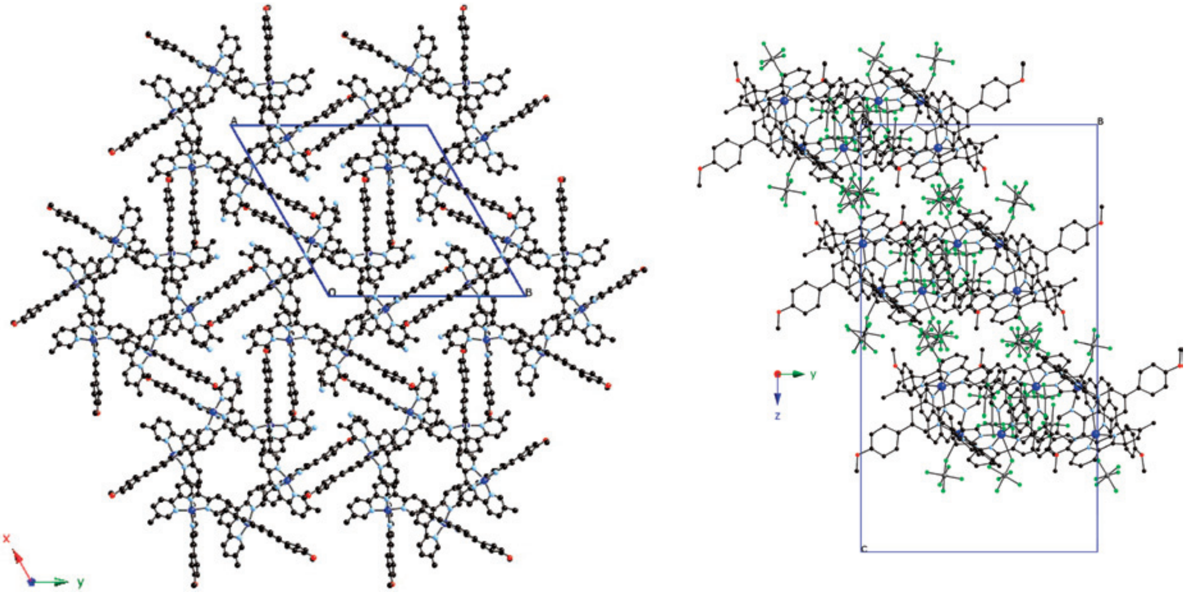

Figure 2. Top view of the [**1**(PF_6)$_6$]$^{6+}$ units hexagonal packing in the *ab* plane. PF_6 anions omitted for clarity (left) and side view showing the packing of the different layers in [**1**][PF_6]$_{12}$ (right).

different ligands in such a way that each copper atom is bound to two ligands and each ligand is bound to two copper atoms, forming a cyclic structure where all of the methoxyphenyl groups are rotating in the same direction. The copper atoms appear alternating above and below the plane with a Cu−Cu−Cu angle of 96(1)°. All of the coordinating PF_6^- anions are located on the outside of the hexamer. The cavity of the ring is occupied by other six noncoordinating PF_6^- anions and solvent molecules, with large crystallographic disorder.

As a consequence of the geometric constraints imposed by the rigidity of **L**, the chelating moieties show slight distortions from perfect planarity, with N1−C5−C6−N2 2.7°, N2−C10−C11−N3 3.50°, and N4−C19−C24−N5 1.40° torsion angles for terpy and phen (Figure 1).

These cations are organized in a typical hexagonal packing, forming layers on the *ab* plane (Figure 2). $\pi-\pi$-stacking interactions between the π-donor methoxyphenyl groups, which are pointing outside the inner cavity and the π-acceptor phen moieties of the neighboring macrocycles (shortest non covalent C−C distance of 3.46(6) Å, average centroid−centroid distance of 3.95(6) Å), very likely contribute to the 2D arrangement of the hexameric cations. The side view of the crystal packing shows a layered stacking with an average separation of 12.83(6) Å. The hexameric cations of adjacent layers are not eclipsed, but with the expected pattern that corresponds to the trigonal space group: each layer showing a 1/3 displacement along the *a* and *b* axes (Figure 2).

DC magnetic susceptibility measurements were performed on a polycrystalline sample of **1**. Experimental data in the 2−300 K range were fitted to Curie−Weiss law, $\chi = C/(T - \Theta) + \mathrm{TIP}$ (TIP $= 3.9 \times 10^{-3}$). The obtained Curie constant value, 2.18 emu mol^{-1}, is in excellent agreement with the expected spin-only value for the sum of noninteracting copper(II) ions ($C_{so} = 2.25$ emu mol^{-1}). The small value of the Weiss constant, $\Theta = -0.3$ K^{-1}, is indicative of the negligible character of magnetic interactions between neighboring $S = {}^1/_2$ spins, in full agreement with the large Cu−Cu distance (8.44 Å) imposed by **L** (Figure 3).

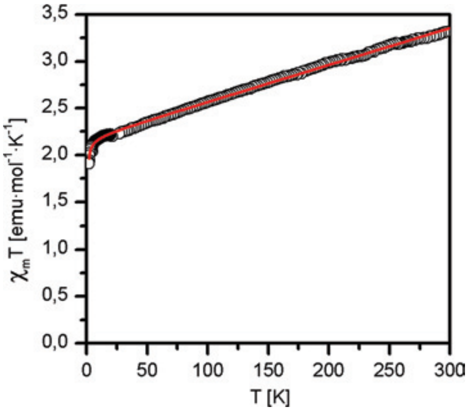

Figure 3. Magnetic susceptibility of the microcrystalline solid obtained by slow evaporation of a 1:1 stoichiometric mixture of **L** and copper(II). Solid red line represents the best fitting to the Curie−Weiss law.

To check the stability of the hexanuclear copper(II) complex [$\mathbf{L}_6Cu_6(PF_6)_6$]$^{6+}$ in solution, we have performed electrospray mass spectrometry (ES-MS). This soft ionization technique has been applied in the characterization of supramolecular entities, and it has been very useful in the structural elucidation of polynuclear transition-metal complexes prepared by self-assembly procedures.[36,37]

Diluted CH_3CN solutions containing 1:1 stoichiometric mixture of **L** and copper(II) (ca. 5×10^{-6} M) have been analyzed by ES-MS at a very low voltage.[38] A very clean spectrum dominated by peaks corresponding to a trinuclear copper(II) complex is obtained. Thus, the major peak (*m*/*z*

---

(36) Schalley, C. A. *Int. J. Mass Spectrom.* **2000**, *194*, 11–39.

(37) Nierengarten, H.; Leize, E.; Breuning, E.; Garcia, A.; Romero-Salguero, F.; Rojo, J.; Lehn, J. M.; Van Dorsselaer, A. *J. Mass Spectrom.* **2002**, *37*, 56–62.

(38) Identical ES mass spectra were observed from solutions obtained by redissolution of the green precipitate in acetonitrile at the same copper concentrations.

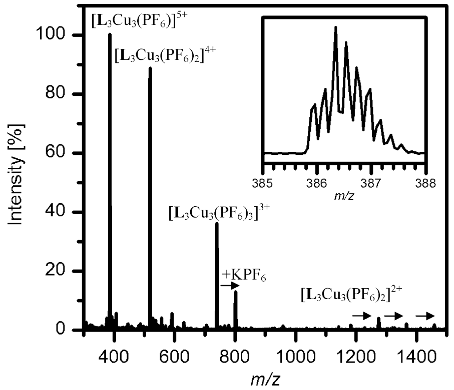

Figure 4. ES-MS of a 1:1 Cu(II)−**L** mixture in CH_3CN (ca. 5 × 10^{-6} M in **L**).

Table 2. Pseudomolecular Peaks in the ES-MS Spectrum of a 1:1 Cu(II)−**L** Mixture in CH_3CN (Diluted Solution) [a]

charge (*z*)	fragment	calcd (*m/z*)	found (*m/z*)
+5	$L_3Cu_3(PF_6)$	386.08	386.01
+4	$L_3Cu_3(PF_6)_2$	518.84	519.02
+3	$L_3Cu_3(PF_6)_3$	740.12	739.84
+3	$L_3Cu_3(PF_6)_3$ + KPF_6	801.47	801.60
+2	$L_3Cu_3(PF_6)_4$	1182.66	1182.75
+2	$L_3Cu_3(PF_6)_4$ + KPF_6	1274.69	1274.90
+2	$L_3Cu_3(PF_6)_4$ + 2 KPF_6	1366.72	1366.59
+2	$L_3Cu_3(PF_6)_4$ + 3 KPF_6	1458.75	1458.85

[a] Cone voltage: 10 V. Positive mode.

= 386.01, Figure 4) has been attributed to a species of formula [$\mathbf{L}_3Cu_3(PF_6)$]$^{5+}$. A series of pseudomolecular peaks corresponding to [$\mathbf{L}_3Cu_3(PF_6)_n$]$^{(6-n)+}$ species formed by addition of hexafluorophosphate anions is observed (Table 2). Unambiguous confirmation of the charge *z* of each peak has been done under high resolution conditions. In all of the cases, a well-resolved isotopic pattern consisting of monoisotopic peaks separated by 1/*z* Da is obtained (inset, Figure 4). Very small peaks attributed to solvated trinuclear [$\mathbf{L}^2Cu_3(CH_3CN)_2(PF_6)_n$]$^{(6\ -\ n)+}$ species formed by loss of ligand have been detected. Finally, several adducts with KPF_6 originating from the metathesis reaction have also been observed.

The hexanuclear copper(II) architecture has not been detected under the experimental conditions. This is probably due to the larger stability of the trinuclear species in diluted conditions. In principle, the stability of complexes of higher nuclearity should increase when increasing the concentration of the sample, and this aspect was also checked by mass spectrometry. A 100-fold increase of the concentration of **1** affords a mass spectrum that is again dominated by the presence of the trinuclear compound. However, new peaks appear that can be ascribed to $\mathbf{L}_2Cu_2$, $\mathbf{L}_4Cu_3$, and $\mathbf{L}_4Cu_4$ species, although no hexanuclear copper(II) complex could still be detected (Figure S2 in the Supporting Information). This attribution has been again checked by high-resolution experiments (inset, Figure S2 in the Supporting Information). In the present case, several adducts with acetate anions originating from the metathesis reaction are observed (Table S1 in the Supporting Information).

Notice that the trinuclear predominant species $\mathbf{L}_3Cu_3$ observed in solution very likely implies a cyclic trimer (a molecular triangle) with an interwoven structure such as that represented in part b of Table 1, in which the linear ditopic ligand adopts a transoid conformation. By contrast, in the hexamer observed in the solid state, the binding sites of the ligand are disposed in a cisoid fashion. Such a change in the ligand conformation may be imposed by the crystal packing of the hexanuclear complex, which is stabilized by $\pi-\pi$ stacking interactions among the neighboring hexamers on the *ab* plane.

The presence of other polynuclear species different from the hexamer observed in the single crystal may be confirmed by X-ray diffraction of the powder obtained by rapid precipitation of a 1:1 stoichiometric mixture of **L** and $Cu(OAc)_2$ in methanol after the addition of an excess of KPF_6. Despite the poor crystallinity of the sample, some peaks are observed in the diffraction pattern, but they are clearly different from those expected for [**1**][PF_6]$_{12}$ single crystals (Figure S3 in the Supporting Information). This result supports the mass spectroscopy studies where species with nuclearity lower than six, mainly three, are found to predominate in acetonitrile solutions.

Finally, the TGA curve of the green powder shows that it is stable up to 120 °C (Figure S4 in the Supporting Information). The weight loss of ~1.9% in the temperature range 120−220 °C could correspond to the loss of 5−6 water molecules in the hexamer. Above ca. 250 °C, the ligand starts to decompose.

Conclusions

We have succeeded in the solid-state self-assembly and structural characterization of metallamacrocycle **1**, the first molecular hexagon of the grid-type family based on a hexanuclear copper(II) complex of a heteroditopic ligand. X-ray crystallography reveals that **1** consists of molecular hexagons in which each metal ion is bound to two different ligands through the phen and terpy units, plus a weakly coordinated PF_6^- anion in a highly distorted octahedral geometry. These cations are organized in a typical hexagonal packing, forming layers on the *ab* plane that are stabilized by $\pi-\pi$ stacking interactions between the π-donor methoxyphenyl groups and the π-acceptor phen moieties of the neighboring metallacycles.

ES-MS studies of acetonitrile solutions of samples obtained by precipitation of 1:1 mixtures of **L** and copper(II) show mixtures of polynuclear complexes of lower nuclearities, in which the trinuclear $\mathbf{L}_3Cu_3$ species is the predominant.

The substitution of copper(II) by other transition metals able to give pentacoordinated complexes is currently under investigation. For instance zinc(II) and cadmium(II) have been tested. However, we have not been able to obtain crystals suitable for X-ray diffraction. ES-MS studies of acetonitrile solutions of the 1:1 stoichiometric mixtures show only the presence of mononuclear species (**L**M and $\mathbf{L}_2$M), whereas ^{1}H NMR spectra in CD_3CN solutions show in both cases broad signals indicative of an equilibrium mixture of different aggregates.

Experimental Section

Physical Measurements. Absorption spectra were recorded on a Shimadzu UV-2501PC spectrophotometer. For the calculation of ϵ, we have considered the trimer as the predominant species in solution. This leads to a concentration of 1.5×10^{-3} M. IR spectra were recorded on a Nicolet 5700 FTIR spectrophotometer as KBr pellets in the 4000−400 cm^{-1} frequency range. ^{1}H NMR spectra were recorded on a Bruker Avance DRX spectrometer at 300 MHz. ES-mass spectra were obtained with a Waters Micromass ZQ spectrometer in the positive ion mode. The extraction cone voltage was set to 10 V to avoid fragmentations. High-resolution mass spectra (FAB) were recorded on a VG-AUTOESPEC spectrometer in the positive ion mode. Magnetic susceptibility measurements were performed on a polycrystalline sample with a Quantum Design MPMS-XL-5 susceptometer equipped with a SQUID sensor. The susceptibility data were corrected from the diamagnetic contributions as deduced by using Pascal's constant tables. DC data were collected in the range 2−300 K with an applied field of 1000 G, and a magnetization curve was acquired up to 5 T at 2 K. Thermogravimetric analysis (TGA) was performed in a Mettler Toledo TGA/SDTA-851 apparatus in the 25−800 °C temperature range under a 30 mL/min flow of air and a heating rate of 10 °C/min.

Crystallographic Analysis. A greenish single crystal of **1** was collected by hand, fixed on a 100 μm MicroMount, and mounted on a Nonius-Kappa CCD single crystal diffractometer equipped with graphite-monochromated Mo Kα radiation ($\lambda = 0.71073$ nm) at 180(2) K. The crystal structure was solved by direct methods using the program *SIR97*,[39] followed by Fourier synthesis and refined on F^2 with *SHELXL-97*.[40] All crystallographic plots were obtained by using the *CrystalMaker* program. All non-hydrogen atoms were located after successive Fourier difference maps. The hydrogen atoms were located in their calculated positions, with their thermal parameters fixed to be 50% larger than those of the atoms to which they are bound. The PF_6^- anions showed disorder regarding the orientation of the fluorine atoms. This disorder was treated by fixing the P−F distances. Different orientations of the octahedra were allowed, resulting in several fluorine atoms with occupancies less than one. Only the heavier atoms, copper and phosphorus, could be refined anisotropically. Several single crystals were assayed, and diffraction intensity was found to be very weak ($\theta_{max} \sim 20.5°$), probably induced by the loss of interstitial solvent molecules. This point did not allow for the obtention of higher quality crystallographic data. CCDC 633699 contains the supplementary crystallographic data for this article.

The X-ray powder profile was collected with a Siemens d-500 X-ray diffractometer (Cu Kα radiation, $\lambda_\alpha = 1.54184$ Å) at 293(2) K. The sample was ground and mounted on a flat sample plate. Typically, profiles were collected as step scans in the $5° < 2\Theta < 50°$ range with a step size of 0.02°. The powder diffraction pattern was simulated with the *Crystal Diffract* software; (*CrystalMaker* software, Oxford, 2006).

Synthesis. Column chromatography was performed with silica gel 60 (230−400 mesh). Silica gel 60 F_{254} (Merck) plates were used for TLC. All reagents were used as purchased without further purification. Toluene was distilled from sodium when required. DMSO was dried over a molecular sieve prior to use. 5-Methyl-2-tributylstannylpyridine,[41] 5-bromo-2-tributylstannylpyridine (**7**),[35] and 3,8-dibromo-1,10-phenanthroline (**4**)[34] were prepared by literature-modified procedures.

6′-Bromo-5-methyl-2,2′-bipyridine (6). 5-Methyl-2-tributylstannylpyridine (4.0 g, 10.5 mmol), 2,5-dibromopyridine (3.79 g, 15.7 mmol), and $Pd(PPh_3)_4$ (0.54 g, 0.47 mmol) were dissolved in toluene (100 mL). The solution was degassed and then refluxed under argon at 120 °C for 2 days. The insoluble precipitate is separated from the warm mixture by filtration. The solvent was evaporated, the resulting solid was dissolved in 2.5 M HCl (100 mL), and the aqueous solution was extracted with CH_2Cl_2. The resulting aqueous phase was basified with concentrated NH_3 at 0 °C to yield a white precipitate. This solid was filtered and purified by column chromatography (silica gel, CH_2Cl_2:MeOH) to yield pure **6** as a white solid (1.56 g, 65%). ^{1}H NMR ($CDCl_3$, 300 MHz): δ 8.48 (d, $J = 2.0$ Hz, 1H), 8.33 (dd, $J = 7.8$ and 0.8 Hz, 1H), 8.29 (d, $J = 8.1$ Hz, 1H), 7.64 (t, $J = 7.8$ Hz, 1H), 7.61 (dd, $J = 8.1$ and 2.0 Hz, 1H), 7.45 (dd, $J = 7.8$ and 0.8 Hz, 1H), 2.93 (s, 3H).

5-Bromo-5″-methyl-2,2′:6′,2″-terpyridine (8). 6′-Bromo-5-methyl-2,2′-bipyridine (**6**; 1.87 g, 7.5 mmol), 5-bromo-2-tributylstannilpyridine (**7**; 3.52 g, 7.88 mmol), and $Pd(PPh_3)_4$ (0.52 g, 0.45 mmol) were dissolved in toluene (200 mL). The solution was degassed and then refluxed under argon at 120 °C for 1 day. The insoluble precipitate formed was separated from the warm mixture by filtration. The solvent was evaporated; the resulting solid was dissolved in 2.5 M HCl (100 mL). The aqueous solution was extracted with CH_2Cl_2 and then it was basified with concentrated NH_3 at 0 °C until the appearance of a white precipitate. The solid was filtered and purified by column chromatography (silica gel, CH_2Cl_2:MeOH) to yield pure **8** as a white solid (2.0 g, 82%). ^{1}H NMR ($CDCl_3$, 300 MHz): δ 8.73 (d, $J = 2.3$ Hz, 1H), 8.55−8.50 (m, 2H), 8.47 (d, $J = 8.1$ Hz, 1H), 8.43 (dd, $J = 7.8$ and 0.9 Hz, 1H), 8.39 (dd, $J = 7.8$ and 0.9 Hz, 1H), 7.96 (dd, $J = 8.5$ and 2.3 Hz, 1H), 7.94 (t, $J = 7.8$ Hz, 1H), 7.66 (dd, $J = 8.1$ and 1.8 Hz, 1H), 2.42 (s, 3H). HRMS(EI): Calcd for $C_{16}H_{12}N_3Br$ 325.021; found 325.023.

5-Neopentyl glicolatoboron-5″-methyl-2,2′:6′,2″-terpyridine (3). A degassed mixture of bromoterpyridine **8** (0.98 g, 3 mmol), bis(neopentyl glycolato)diboron (0.77 g, 3.3 mmol), and $PdCl_2$(dppf) (0.073 g, 0.09 mmol) in anhydrous DMSO (15 mL) was stirred at 80 °C for 5 h. CH_2Cl_2 (100 mL) was then added, and the organic phase was washed with H_2O and dried over Na_2SO_4. The solvent was evaporated under reduced pressure and the resulting solid was crystallized from EtOH/CH_2Cl_2 to yield pure **3** as a white solid (0.70 g, 65%). ^{1}H NMR ($CDCl_3$, 300 MHz): δ 8.98 (s, 1H), 8.55−8.40 (m, 4H), 8.37 (d, $J = 7.8$ Hz, 1H), 8.18 (dd, $J = 7.9$ and 1.4 Hz, 1H), 7.89 (d, $J = 7.8$ Hz, 1H), 7.63 (dd, $J = 8.1$ and 1.9 Hz, 1H), 3.75 (s, 4H), 2.35 (s, 3H), 0.99 (s, 6H).

3-Bromo-8-(p-methoxyphenyl)-1,10-phenanthroline (2). A degassed 2 M Na_2CO_3 aqueous solution was added via a cannula to a mixture of 3,8-dibromo-1,10-phenanthroline (**4**; 2.0 g, 5.92 mmol), 4-methoxyphenylboronic acid neopentylglycol ester (**5**; 1.18 g, 5.36 mmol), and $Pd(PPh_3)_4$ (0.32 g, 0.28 mmol) in toluene (100 mL). The mixture was degassed again and refluxed under argon at 120 °C for 24 h. Then, 100 mL of water was added. The organic layer was separated, and the aqueous layer was extracted with $CHCl_3$. The combined organic phases were washed once again with water. They were then dried over Na_2SO_4, and the solvent was evaporated under reduced pressure to afford the crude product. Chromatography on silica column using CH_2Cl_2/AcOEt as eluent provided the desired monosubstituted product **2** as a white solid (1.10 g, 56%). ^{1}H NMR

---

(39) Altomare, A.; Burla, M. C.; Camalli, M.; Cascarano, G. L.; Giacovazzo, C.; Guagliardi, A.; Moliterni, A. G. G.; Polidori, G.; Spagna, R. J. *Appl. Crystallogr.* **1999**, *32*, 115–119.

(40) Sheldrick, G. M. in *SHELXL-97: Programs for Crystal Structure Analysis*; University of Göttingen: Göttingen, Germany 1997.

(41) Schubert, U. S.; Eschbaumer, C.; Hochwimmer, G. *Synthesis* **1999**, 779–782.

($CDCl_3$, 300 MHz): δ 9.39 (d, $J = 2.3$ Hz, 1H) 9.17 (d, $J = 2.3$ Hz, 1H), 8.39 (d, $J = 2.3$ Hz, 1H), 8.32 (d, $J = 2.3$ Hz, 1H), 7.86 (d, $J = 8.8$ Hz, 1H), 7.74−7.68 (m, 3H), 7.08 (d, $J = 8.8$ 2H), 3.89 (s, 3H). HRMS(FAB): Calcd for $C_{20}H_{13}N_2OBr$ 364.010; found 364.010.

Ligand L. Bromophenanthroline **2** (0.73 g, 2.00 mmol), boronic ester derivative **3** (0.72 g, 2.00 mmol), $Pd[P(Ph)_3]_4$ (0.17 g, 0.15 mmol), K_2CO_3(2.76 g, 20 mmol), DMF (60 mL), and water (2 mL) were degassed and heated under argon at 80 °C for 18 h. The resulting solid was filtrated and washed with 10 mL of a 8:2 DMF/CH_2Cl_2 mixture, then water (25 mL), 1.5 M HCl (50 mL), concentrated NH_3 (50 mL), and water again (25 mL). The solid was dried in vacuo and used without further purification (white solid, 0.71 g, 67%). ^{1}H NMR ($CDCl_3$, 300 MHz): δ 9.5 (d, $J =$ 2.3 Hz, 1H), 9.44 (d, $J = 2.3$ Hz, 1H), 9.12 (d, $J = 2.0$ Hz, 1H), 8.82 (d, $J = 8.3$ Hz, 1H), 8.59−8.43 (m, 5H), 8.37 (d, $J = 2.3$ Hz, 1H), 8.26 (dd, $J = 8.3$ and 2.4 Hz, 1H), 7.99 (t, $J = 7.8$ Hz, 1H), 7.92 (s, 2H), 7.74 (d, $J = 8.7$ Hz, 2H), 7.70 (s, 1H), 7.10 (d, $J =$ 8.7 Hz, 2H), 3.91 (s, 3H) 2.44 (s, 3H). HRMS(FAB): Calcd for $C_{35}H_{25}N_5O$ 531.206; found 531.205.

$[Cu_6(L)_6(PF_6)_6](PF_6)_6$ ([1][PF_6]$_{12}$). A mixture of **L** (53 mg, 0.1 mmol) and $Cu(OAc)_2$ (18 mg, 0.1 mmol) were stirred in MeOH (10 mL) for 30 min. Then, 5 equiv of KPF_6 in 5 mL of water were added. The MeOH was evaporated under reduced pressure, and the resulting precipitate was collected by filtration to yield a green powder in quantitative yield. IR (KBr): $\nu = 1605$ (s), 1520 (m), 1439 (s), 1252 (s), 841 (vs) and 558 (s) cm^{-1}. UV−vis (MeOH): $\lambda_{max} = 650$ nm ($\epsilon = 322 \cdot M^{-1} \cdot cm^{-1}$) (Figure S4 in the Supporting Information). This broadband can be assigned to a d−d metal-centered transition, as expected for a copper(II) 5-coordinated species complexed by a terpy and a phen units.[42,43] Anal. Calcd for $C_{210}H_{162}Cu_6N_{30}O_{12}P_{12}F_{72}$: C, 46.55; H, 3.01; N, 7.75. Found: C. 46.6; H, 3.1; N, 7.6.

Single crystals suitable for X-ray analysis were obtained by slow evaporation of an acetonitrile solution containing the green precipitate. Some polycrystalline green powder was also obtained. Crystal data for $([Cu(C_{35}H_{25}N_5O)(PF_6)][PF_6])_6 \cdot 9H_2O \cdot 9CH_3CN$: $C_{228}H_{195}Cu_6F_{72}N_{39}O_{15}P_{12}$, M = 5842.11, trigonal, $R\bar{3}$, $a = 24.651(2)$, $c = 38.492(3)$ Å, $V = 20257(3)$ Å^3, $T = 180$ K, $Z = 3$, $m = 0.647$ mm-1, 11 971 reflections (6270 unique, $R_{int} = 0.4218$) with 6.36° $< 2\theta <$ 50.12°, 310 variables, $R = 0.0979$, $wR(F_o^2) = 0.2074$[1536 data, $I > 3s(I)$], GOF = 0.719. CCDC 633699 contains the supplementary crystallographic data for this article.

Supporting Information. Figures of polyhedral representation of the copper coordination, ES-MS and UV−vis spectra of a concentrated stoichiometric mixture of **L** and $Cu(OAc)_2$ in methanol, X-ray powder diffraction spectra and TGA curve of the green polycrystalline solid, and a table of peak assignments. This material is available free of charge via the Internet at http://pubs.acs.org. Also, see http://dx.doi.org/10.1039/b000000x/.

Acknowledgment. Financial support from the European Union (NoE MAGMANet, NMP3-CT2005-515767), the Spanish Ministerio de Educación y Ciencia (CONSOLIDER-INGENIO 2010, CSD2007-00010, and project MAT2004-03849), and the Generalitat Valenciana are gratefully acknowledged. S.T. thanks the MEC for a predoctoral fellowship.

IC8000569

---

(42) Hasenknopf, B.; Lehn, J. M.; Baum, G.; Fenske, D. *Proc. Natl. Acad. Sci. U.S.A.* **1996**, *93*, 1397–1400.

(43) Hamann, C.; Kern, J. M.; Sauvage, J. P. *Inorg. Chem.* **2003**, *42*, 1877–1883.